09.7;07.2

Development and study of a model of an autonomous energy information station of free space optical communication

© V.S. Kalinovskii, E.I. Terukov, Yu.V. Ascheulov, E.V. Kontrosh, V.S. Yuferev, K.K. Prudchenko, A.V. Chekalin, E.E. Terukova, I.A. Tolkachev, S.E. Goncharov, V.M. Ustinov

Ioffe Institute, St. Petersburg, Russia
E-mail: vitak.sopt@mail.ioffe.ru

Received July 12, 2022
Revised November 10, 2022
Accepted November 14, 2022

A model of an autonomous receiving station of free space optical communication system based on a multi-section energy heterostructure (HJT) Si photoconverter and an information photodetector based on AlGaAs/GaAs $p-i-n$ photodiodes has been developed. The energy part, when excited by laser radiation with a power of ~ 264 W at a wavelength of 0.974 μm in the photovoltaic mode, provided $\geqslant 60$ W of electric power. The photodetector of the information channel, when excited by pulsed radiation at a wavelength of 0.78 μm, provides response time in the photovoltaic mode in the sub-nanosecond range.

Keywords: free space opical communication, receiving station, HJT Si photoconverter, AlGaAs/GaAs $p-i-n$ photodetector, laser radiation, pulsed radiation

DOI: 10.21883/TPL.2023.01.55352.19306

Free-space optical communication (FSO) [1] is needed to establish high-speed wireless information channels both in urban centers and in remote regions for instant communication [2–5]. FSO is generally used to „extend" fixed communication lines within the „last mile" when a secure duplex channel is needed. In this scenario, one transmitting-and-receiving FSO station is provided with a permanent power supply, while the other (located at the remote line end) is not; therefore, the problem of reliable and long-term operation of this second station arises. Transmitting-and-receiving FSO stations produced in Russia [6,7] and abroad [1–5] normally feature a modulated radiation source for laser information transmission and a high-speed laser photodetector for receiving the response signal from the other station of a duplex channel. These systems have no additional built-in photoconverters for reception of free-space laser radiation needed to provide power supply for a transmitter-receiver station. In the present study, we propose for the first time a novel design of autonomous FSO stations of this kind that utilize hybrid photoconverters based on α-Si:H/Si photovoltaic converters (PVCs), which convert high-power laser radiation with wavelength λ_1 within the atmospheric transparency window, and nanoheterostructure A_3B_5 PVCs for the information channel operating at wavelength λ_2, where $\lambda_1 \neq \lambda_2$. Hybrid PVCs provide power supply for transmitting-and-receiving FSO station channels.

The results of examination of parameters of a model autonomous multi-section receiving FSO station, which features an energy channel with heterostructure (HJT) PVCs and an information channel with AlGaAs/GaAs $p-i-n$ photodiodes operating in the photovoltaic mode at wavelengths of 0.974 and 0.78 μm, respectively, are reported below.

This model (Fig. 1, *a*) is comprised of a multi-section energy photoconverter device (MEPD) and an information AlGaAs/GaAs $p-i-n$ photodetector (PD) operated simultaneously in the photovoltaic mode.

The MEPD was constructed from HJT elements 15.6×15.6 cm in size (Fig. 1, *a*). HJT PVCs were fabricated by plasma-enhanced chemical vapor deposition (PECVD) on a textured *n*-type *c*-Si substrate [8]. Indium tin oxide (ITO) layers were formed next by physical vapor deposition (PVD). Contact Ag buses were formed by screen printing on the surface of ITO layers. The model MEPD features central (with 16 elements connected in series) and periphery (with 12 HJT elements connected in series) modules. Bypass diodes (28 in total) were connected oppositely in parallel to each element.

The information PD was fabricated based on four AlGaAs/GaAs $p-i-n$ photodiodes connected in series with a photoactive surface diameter of 500 μm. The epitaxial heterostructure of these photodiodes was grown by molecular beam epitaxy [9] and contained a GaAs $p-i-n$ junction, a wide-band window, and a back potential barrier based on an $Al_xGa_{1-x}As$ solid solution. The electric wiring and mounting of $p-i-n$ photodiodes were performed on an AlN heat-sink base. Silicon lenses were formed on the photoactive surface of photodiodes. The information PD with an aluminum optical concentrator (focon) was mounted directly at the center of the photosensitive surface of the energy MEPD (Fig. 1, *a*).

Photovoltaic parameters of the model FSO were measured under combined illumination by continuous wave (CW) laser radiation with a wavelength of 0.974 μm and a power up to 264 W and pulsed laser radiation with a wavelength of 0.78 μm, an average power up to 120 mW, a

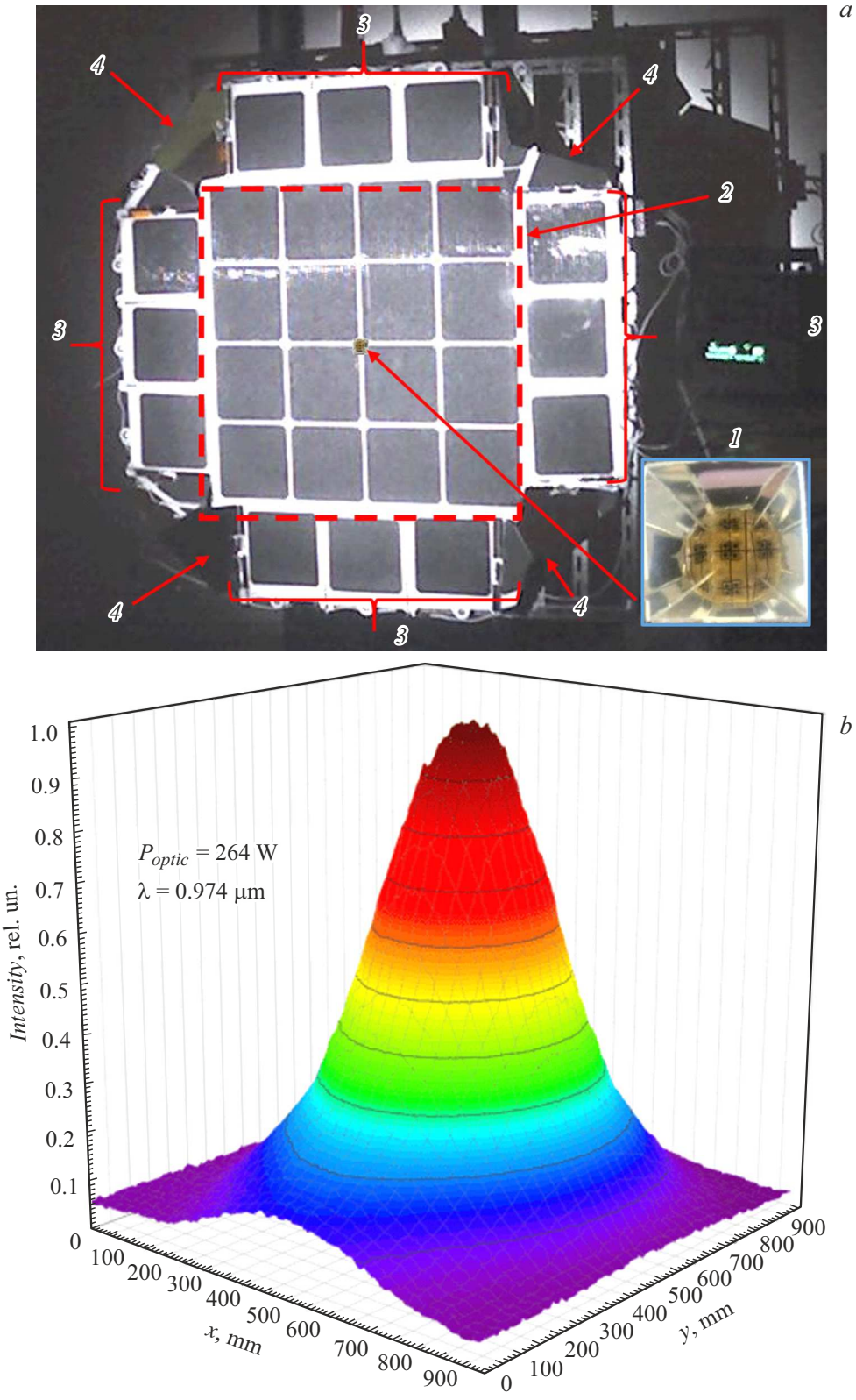

Figure 1. *a* — Photographic image of the model of an autonomous energy and information receiving station for free-space optical communication: information AlGaAs/GaAs $p-i-n$ PD (*1*), central (*2*) and periphery (*3*) MEPD modules comprised of HJT PVCs, and Al angle reflectors (*4*); *b* — intensity distribution of laser radiation with a power of 264 W ($\lambda = 0.974\,\mu$m) on the MEPD surface; *c* — temperature distribution on the front face of the model MEPD in the CW radiation mode at a power of 264 W ($\lambda = 0.974\,\mu$m).

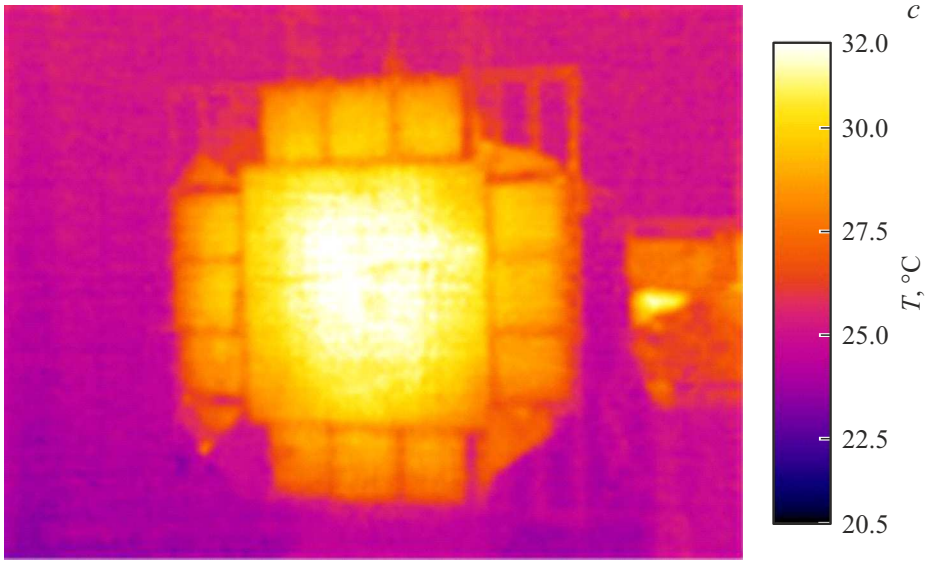

Fig. 1 (*continued*).

half-amplitude duration of $\leqslant 10$ ps, and a repetition rate of 71 MHz. In order to simulate the divergence of laser radiation in atmosphere, these measurements were performed with the use of optical fiber. The fiber core diameter in the information ($0.78\,\mu$m) and energy ($0.974\,\mu$m) channels was 200 and $135\,\mu$m, respectively. The divergence angle of laser radiation at the fiber output was $\geqslant 10°$. Figure 1, *b* presents the intensity distribution of laser radiation of the energy channel on the MEPD surface. The heat distribution on the MEPD surface under CW laser irradiation is shown in Fig. 1, *c*. According to the temperature distribution under irradiation ($0.974\,\mu$m) with a power of 264 W, the peak PVC temperature was $\sim 32°$C.

The spectral sensitivity of AlGaAs/GaAs $p-i-n$ photodiodes and HJT elements fell within the range of 0.7–$0.9\,\mu$m and 0.4–$1.1\,\mu$m, respectively. The external quantum efficiency of photodiodes at the information signal wavelength ($0.78\,\mu$m) and HJT elements at the energy signal wavelength ($0.974\,\mu$m) was $\sim 90\%$.

The photoresponse pulse parameters of the information PD were measured in the photovoltaic mode. The determined photoresponse pulse shapes and time parameters are presented in Figs. 2, *a*, *b*. According to the obtained results, the signal pulse amplitude at a load of $50\,\Omega$ decreases by 60% as the laser spot area increases from 0.2 to $2\,\text{cm}^2$; in contrast to amplitude, the time parameters remain essentially unchanged. The following values were determined for a laser spot area of $2\,\text{cm}^2$: signal pulse amplitude at a load of $50\,\Omega$ — 18 mV, pulse rise time $\tau_{rise} = 0.18$ ns, fall time $\tau_{fall} = 2.6$ ns, and half-amplitude pulse duration $\tau_{0.5} = 730$ ps (Fig. 2).

Figure 3 shows calculated and experimental load current–voltage characteristics (l–V) of the MEPD under excitation by laser radiation with a wavelength of $0.974\,\mu$m. Experimental dark characteristics of an individual HJT element were used to simulate load curves. It turned out that the only way to achieve a fine agreement between calculated and experimental light l–V for an HJT element is to reduce the contact resistance (determined by fitting the dark l–V) to $1.2\,\Omega \cdot \text{cm}^2$. The distribution of laser radiation intensity over the MEPD surface had a near-Gaussian shape (Fig. 1, *b*). It was assumed in calculations of light l–V that the current density at each point of an HJT element is defined by the local radiation intensity at this point and the applied voltage (i.e., does not depend on the current at neighboring points). It can be seen from Fig. 3 that the load curves for the central MEPD module agree fairly closely, while the differences in open-circuit voltage U_{oc} and the maximum power for periphery modules are rather significant. These discrepancies are attributable to the fact that the laser radiation intensity in the region of periphery modules deviates considerably (upward) from the „traditional" Gaussian distribution used in calculations. The resulting calculated maximum electric power is 54 W, which is 10% lower than the experimental value. It is also necessary to point out that, owing to a reduced intensity of illumination of periphery modules, the MEPD current decreases with increasing voltage much faster than the central module current; this translates into a reduction in U_{oc} and a lower conversion efficiency. Note that in the case of, e.g., parallel connection of central and periphery modules and nonuniform illumination, currents within the MEPD in the indicated modules are nonzero even in no-load operation and close on each other.

According to the measured light l–V, the maximum experimental direct electric power produced was $\geqslant 60$ W at a laser radiation power of 264 W ($\lambda = 0.974\,\mu$m) and parallel connection of central and periphery modules. The efficiency determined with and without regard for optical losses at interelement non-photoactive regions of the pe-

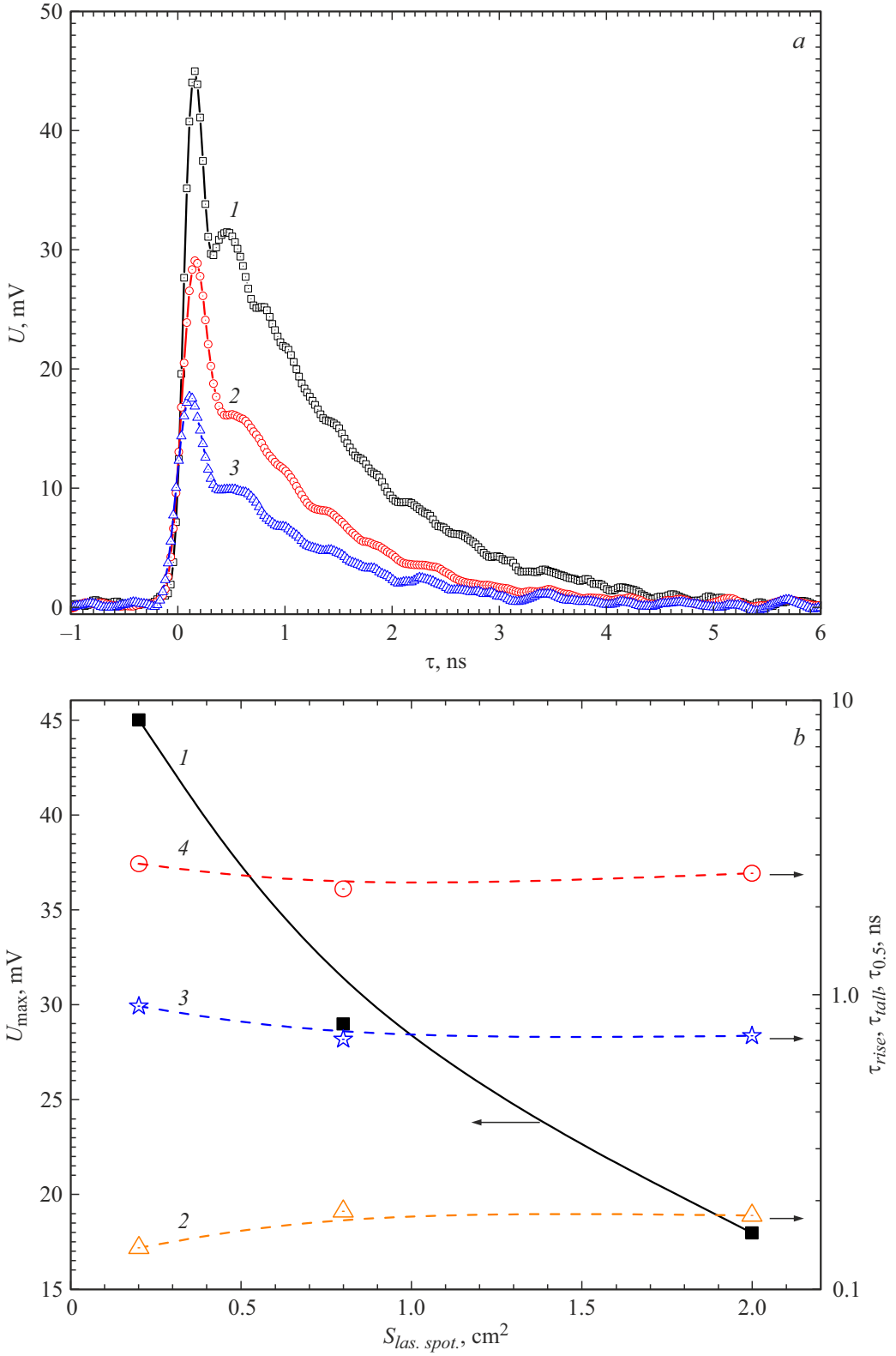

Figure 2. *a* — Photoresponse pulses of the AlGaAs/GaAs $p-i-n$ PD with a focon for a laser radiation spot 0.2 (*1*), 0.8 (*2*), and 2 cm^2 (*3* in size); *b* — dependences of maximum pulse amplitude $U_{\max}$ (*1*), rise time τ_{rise} (*2*), half-amplitude pulse duration $\tau_{0.5}$ (*3*), and fall time τ_{fall} (*4*) on the laser radiation spot size ($\lambda = 0.78\,\mu$m) at the input of the information PD.

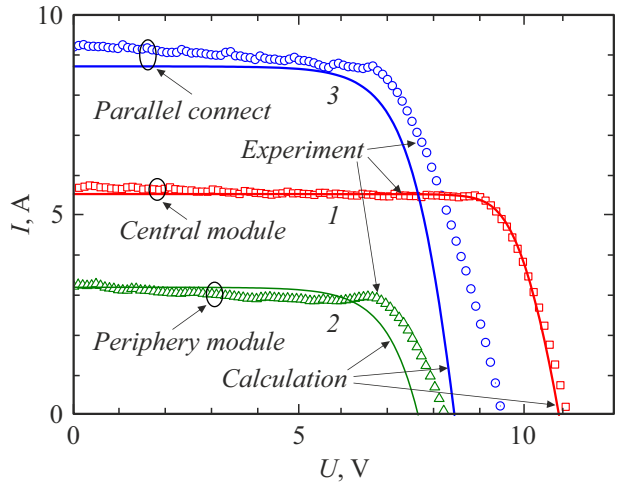

Figure 3. Experimental and calculated light I–V of the model MEPD under excitation by laser radiation with wavelength $\lambda = 0.974\,\mu$m and a power of 264 W. *1* — Central module, *2* — periphery module, *3* — parallel connection of these modules.

riphery module of the model is then $\geqslant 25\%$ and $\sim 22.7\%$, respectively.

A model autonomous energy and information receiving FSO station with a multi-section photoconverter device based on α-Si:H/c-Si PVCs and AlGaAs/GaAs $p-i-n$ PDs has been designed and fabricated for the first time. In the photovoltaic mode, this model has the capacity for simultaneous conversion of CW laser radiation (wavelength — of $0.974\,\mu$m, power — ~ 264 W) with an efficiency of $\sim 25.0\%$ and reception of pulsed monochromatic radiation ($0.78\,\mu$m) with a half-amplitude photoresponse duration of $\leqslant 900$ ps.

Funding

This study was supported financially by the Ministry of Science and Higher Education of the Russian Federation.

Conflict of interest

The authors declare that they have no conflict of interest.

References

[1] M. Garlińska, A. Pręgowska, K. Masztalerz, M. Osial, Future Internet, **12**, 179 (2020). DOI: 10.3390/fi12110179
[2] A.J. Aljohani, J. Mirza, S. Ghafoor, IEEE Commun. Lett., **25**, 196 (2021). DOI: 10.1109/LCOMM.2020.3029591
[3] R. Miglani, J.S. Malhotra, A.R. Majumdar, F. Tubbal, R. Raad, IEEE Photon. J., **12**, 7904621 (2020). DOI: 10.1109/JPHOT.2020.3013525
[4] M.S. Khan, S. Ghafoor, J. Mirza, S.M. Hassan Zaidi, in *2019 IEEE 16th Int. Conf. on smart cities: improving quality of life using ICT & IoT and AI (HONET-ICT)* (IEEE, 2019), p. 074–079. DOI: 10.1109/HONET.2019.8908077
[5] S. Liverman, H. Bialek, A.S. Natarajan, A.X. Wang, J. Lightwave Technol., **38**, 1659 (2020). DOI: 10.1109/JLT.2019.2958733
[6] A.A. Boev, M.Yu. Kernosov, S.N. Kuznetsov, B.I. Ognev, A.A. Parshin, Vestn. Ryazan. Gos. Radiotekh. Univ., **62** (4), 44 (2017) (in Russian). DOI: 10.21667/1995-4565-2017-62-4-44-48
[7] S. Kuznetsov, B.I. Ognev, S. Polyakov, S. Yurko, SPIE Newsroom (2014). DOI: 10.1117/2.1201405.005486
[8] A.S. Abramov, D.A. Andronikov, S.N. Abolmasov, E.I. Terukov, in *High-efficient low-cost photovoltaics*, ed. by V. Petrova-Koch, R. Hezel, A. Goetzberger, Springer Ser. in Optical Sciences (Springer, Cham, 2020), vol. 140, p. 113–132. DOI: 10.1007/978-3-030-22864-4_7
[9] V.S. Kalinovskii, E.V. Kontrosh, G.V. Klimko, T.S. Tabarov, S.V. Ivanov, V.M. Andreev, Tech. Phys. Lett., **44**, 1013 (2018). DOI: 10.1134/S1063785018110214.